Momentum losses by charge exchange with neutral particles in H-mode discharges at JET

T.W. Versloot[1*], P.C. de Vries[1,2], C. Giroud[2], M. Brix[2], M.G. von Hellermann[1], D. Moulton[3], M.O' Mullane[4], A. Salmi[5], T. Tala[6], I. Voitsekhovich[2], K.-D. Zastrow[2] and JET-EFDA Contributors†

JET-EFDA Culham Science Centre, Abingdon, OX14 3DB, UK
[1] FOM Institute Rijnhuizen, Association EURATOM-FOM, Nieuwegein, the Netherlands
[2] EURATOM/CCFE Fusion Association, Culham Science Centre, Abingdon, UK
[3] Imperial College of Science, Technology and Medicine, London, UK
[4] Department of Physics and Applied Physics, University of Strathclyde, Glasgow, G4 0NG, UK
[5] Association EURAROM-Tekes, HUT, P.O. Box 4100, 02015 TKK, Finland
[6] Association EURATOM-Tekes VTT, P.P. Box 1000, 02044 VTT, Finland

1. Introduction

Extensive investigations both in theory and experiments have been done in recent years to identify the influence of rotation on plasma performance. Results have shown that a radial velocity gradient can play a role in the suppression of turbulent transport and profile stiffness [1]. It remains however largely unknown what processes determine the shape and magnitude of the observed rotation profile. With the presence of an inwards momentum pinch [2], the edge momentum density is observed to contribute significantly to the global confinement [3]. Therefore, in order to accurately predict the observed rotation profile, a better understanding of the processes that determine the edge rotation is needed.

Several components play a role in momentum transport in the edge. The dominant source of torque at JET is provided by NBI, while radial transport by outwards diffusivity and an inwards convective pinch redistribute the momentum density. At the edge, a continuous sink is present in the form of charge-exchange (CX) interactions between plasma ions and a neutral particle background. Besides these direct losses, the penetration of low energy neutrals into the plasma periphery is also believed to play a role in several plasma models related to the pedestal shape [4] and the L-H transition [5]. In this paper, the results from a qualitative neutral transport model are used to assess the penetration of neutral atoms into the plasma edge. A forward model of the passive charge-exchange emission [6] is used in order to quantify the neutral density and to estimate the magnitude of momentum and energy losses by CX interactions.

2. Experiments

A series of discharges was selected with a similar plasma configuration and equal external heating powers, but increasing input gas flux during the flat top H-mode period. The heating and torque deposition was majorly supplied by NBI at P_{TOT}=15(±1)MW and T_{NBI}=16(±1)Nm in discharges with a plasma current of I_p=2.5MA and toroidal field of B_T=2.7T. The gas-influx (Γ_g) was supplied by ring valves located at the inner divertor and increased from non-fuelled to a

* E-mail: Thijs.Versloot@ccfe.ac.uk
† See the Appendix of F. Romanelli et al., Proceedings of the 22nd IAEA Fusion Energy Conference, Geneva, Switzerland, 2008

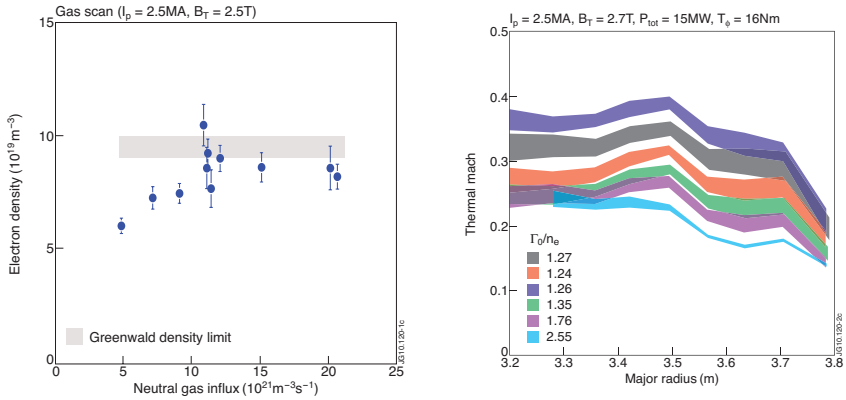

Figure 1: *(a) Volume averaged electron density and limit versus the neutral flux through the LCFS as obtained from the 1D neutral model. (b) Thermal mach profile ($M_{th}=\omega_\varphi R/v_{th}$) for all discharges, showing a global drop in the mach profile with increasing neutral influx*

maximum of $\Gamma_{g,max}$~4x10^{22} elec/s at high triangularity (δ~0.40-0.44). Immediately it was observed that the ELM behaviour changes dramatically with external fuelling**.** A regular ELM period (f_{ELM}~10Hz) is observed in the non-fuelled case, while with increased fuelling the ELM behaviour becomes less pronounce with an increase in the baseline D_α-radiation and ELM frequency. Higher edge electron densities (n_e) are observed with higher rates of gas dosing (see figure 1a) as also studied in [7]. The total thermal angular momentum is obtained from volume integrating the momentum density ($l_\varphi = n_i m v_\varphi$) obtained using the core CXRS diagnostic. The ion species measured is that of the main impurity, C^{5+}, and it is assumed that all the ion species are in equilibrium. For this analysis, the magnitude and shape of n_e and T_e at the pedestal is of high importance for correctly modelling the neutral density profile as well as to forward model the passive CX emission. High resolution Li-beam data is used in combination with Thomson Scattering to obtain the ELM averaged profile. The electron temperature (T_e) profile is obtained from Electron Cyclotron Emission. Both ion temperature and rotation velocity are observed to decrease as the electron density increases during the gas scan. A significant drop in thermal Mach number over the full profile is visible in figure 1b. The angular momentum (L_φ) and total thermal energy (W_{th}) decrease with gas flux under equal heating conditions. This reduction is mostly originating from a decrease at the pedestal where also the confinement properties are degrading. In comparison with the non-fuelled case, the fraction of angular momentum at $\Gamma_{g,max}$ is 0.50 (±0.07) compared to 0.67(±0.08) for the total thermal energy (see also figure 3a). Both the energy confinement time and momentum confinement time drop but it is interesting to note that their ratio ($R_\tau = \tau_E/\tau_\varphi$) increases slightly, see figure 3b, suggesting a different behaviour between momentum and energy losses in the presence of a neutral background.

3. Neutral Particle Dynamics

In general, the plasma is considered to be impermeable to neutrals with the penetration depth limited to a few cm [8]. Neutral particles are unbound by the magnetic field and multiple interactions can redistribute energy, particles and momentum. At each CX interaction, the plasma

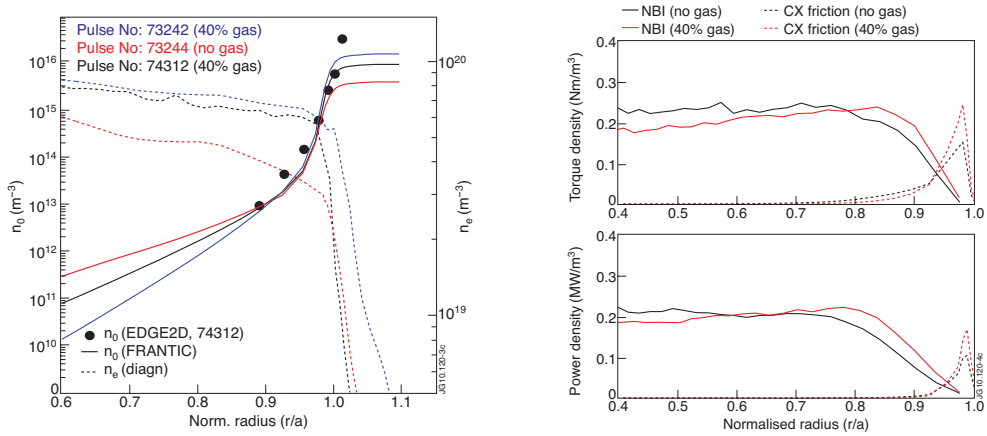

Figure 2: *(a) Neutral (full) and electron (dashed) density profiles for non-fuelled and maximum fuelled discharges. For comparison, the neutral density from a 2D simulation code (EDGE2D-EIRENE) is plotted, showing a good agreement with the 1D neutral transport response after adjustment with PCX. (b) Beam torque (top) and power (bottom) deposition profile and charge-exchange friction components (shown as positive)*

ion and neutral swap identities. This process is considered to be a soft interaction [9] where the outgoing neutral obtains a velocity characterised by the local ion temperature. Energy, a scalar quantity, can be subsequently regained by the plasma in secondary interactions while momentum transferred to the neutral fluid is assumed completely lost to either the wall or by viscous dissipation [10]. Hence multiple CX interactions will constitute a difference in momentum and energy losses. To determine the magnitude of CX losses, the neutral density is modelled in this paper using a simple 1D model [11-12] by determining the neutral transport response of the plasma. The neutral population was split in two contributions with their relative intensity and energy obtained from visible Bremsstrahlung measurements (n^0_{hot}[0.35,10eV], n^0_{cold}[0.6,1eV]). The modelled neutral penetration was then calibrated by forward modelling the passive charge-exchange emission (PCX) and comparing the obtained emission profile to the measured photon flux for all mid-plane CXRS lines of sight. Figure 2a shows the adjusted n_0 profiles for two discharges as well as the poloidal averaged neutral density from a 2D edge model (EDGE2D-EIRENE) for comparison [13]. With increasing neutral influx, the edge electron density increases, shielding the core plasma from penetration from cold neutrals. The obtained neutral density is found in both cases of similar order of magnitude at the plasma edge, $n_0(r/a=1.0) \sim O(10^{15\text{-}16})m^{-3}$.

4. Momentum and Energy Losses

Using the obtained neutral density profile, figure 2b shows the calculated charge-exchange friction ($mn_in_0\langle v\sigma\rangle(v_\varphi-v_0)$) and power loss ($n_in_0\langle v\sigma\rangle(T_i-T_0)$) [8]. Due to the increase in n_e the beam deposition has shifted outwards. The magnitude of CX friction drops rapidly, but is seen to be present up to r/a~0.9 with the torque density being larger than the power loss density. The CX losses are similar in magnitude to the local beam deposition at the edge. In figure 3a, W_{th} and L_φ of all discharges are shown normalised to the non-fuelled case. A decrease is observed as the confinement degrades but with a larger reduction in L_φ. The magnitude of CX losses increases to approximately 10% of the total input torque with the power losses being smaller (<3%).

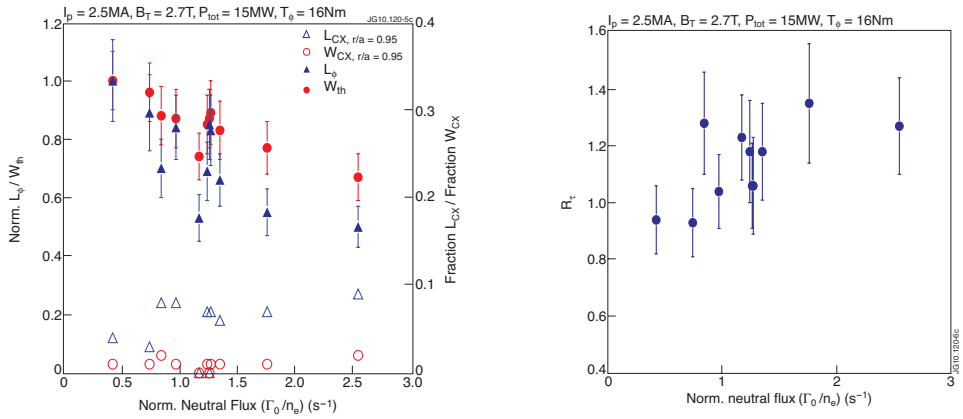

Figure 3: *(a) W_{th} (circles) and L_ϕ (triangles) normalised to a reference discharge without external fuelling. Open symbols refer to the charge-exchange losses using the calibrated neutral density profile and integrated up to 95% of the plasma radius (b) Confinement time ratio as a function of total normalised neutral influx*

5. Conclusions

It was found that the magnitude of charge-exchange losses for momentum and energy differ when comparing discharges at low and high gas dosing. An increase in friction losses is observed up to 10% of the total input torque with the power losses appearing smaller. This behaviour is consistent with the presence of multiple CX interactions within the main plasma causing additional losses of momentum compared to energy. The uncertainty on the absolute magnitude remains large and more detailed neutral transport calculations are required to fully quantify the losses [14]. Also, other loss and transport processes which effect the pedestal and confinement have been excluded, however the increase in frictional losses does suggest a direct link between external conditions and global observed confinement. Atomic physics processes can thus play a direct role in setting the necessary boundary conditions and therefore need to be taken into account when predicting global plasma properties.

This work, supported by the European Communities under the contract of Association between EURATOM and FOM and CCFE, was carried out within the framework of the European Fusion Development Agreement. The views and opinions expressed herein do not necessarily reflect those of the European Commission.

References

[1] Mantica P. *et al.,Phys. Rev. Lett.*, **102**, 175002, (2009)
[2] Tala T., *et al.*, *Plasma Phys. Control. Fusion,* **49**, B291 (2007)
[3] de Vries P.C. *et al., Plasma Phys. Control Fusion,* **52**, 065004 (2010)
[4] Mahdavi, *et. el, Phys. Plasmas*, **10**, p3984 (2003)
[5] Owen L.W., *et. al, Plasma. Phys. Control. Fusion*, **40**, p717 (1998)
[6] Tunklev M., *et. al., Plasma Phys. Control. Fusion*, **41**, 985-1004 (1999)
[7] Maddison G., *et al. Proc. 19th PSI Conference*, San Diego, 2010
[8] Carreras B.A., *et al. Phys. Plasmas*, **3**, 11, 4106-4114 (1996)
[9] Tendler M., *et al., Fusion Technology*, **11**, 289-310 (1987)
[10] Hazeltine R.D., *et al., Nucl. Fusion*, **32**, 3-14 (1992)
[11] S. Tomar, *Journal of Comp. Phys.* **40**, 104-119, (1981)
[12] Valovic M., *et al., Plasma Phys. Control. Fusion*, **46**, 1877-1889 (2004)
[13] Moulton D., *et al., Proc. 19th PSI Conference*, San Diego, 2010
[14] Friis Z.W., *et al., Phys. Plasmas*, **17**, 022507 (2010)